TRACKING MAXIMUM POWER POINT BASED ON IMPROVED SLIDING MODE FOR WIND ENERGY CONVERSION SYSTEMS

Le Xuan Chau[1], Le Kim Hung[2], Minh Quan Duong[2]*

[1]*Naval Academy, Khanh Hoa province, Vietnam*

[2]*The University of Danang - University of Science and Technology, Danang, Vietnam*

*Corresponding author: dmquan@dut.udn.vn

(Received: May 05, 2025; Revised: June 15, 2025; Accepted: June 22, 2025)

DOI: 10.31130/ud-jst.2025.23(9C).548E

Abstract - In the era of net zero emissions for nations worldwide, wind power energy conversion systems-which use clean and incredibly large wind energy reserves to generate electricity-have become popular. The generator of wind turbines is crucial to the process of converting mechanical energy into electrical energy, and because wind is unpredictable, a control system is required to monitor the maximum power of wind turbines. Therefore, in this study, a mode free (MFC) sliding mode control (SMC) is proposed to adhere to track maximum power point for the permanent magnet generator (PMSG) and the MATLAB simulation results are compared with linear quadratic regulator (LQR) to evaluate the working efficiency of the proposed controller applied to WECS.

Key words - Free model control; sliding mode control; wind energy conversion system; linear quadratic regulator

1. Introduction

Wind energy conversation system (WECS) is quite complex in terms of system structure, with interwoven mechanical and electrical parameters that interact with each other. Therefore, the parameters are all described in nonlinear form, necessitating control solutions that effectively address the nonlinear issues. The related publications on control solutions for WECS are divided into two groups: conventional algorithm controller and intelligent algorithm controller [1]. In the group of traditional algorithms, they apply mechanical sensors, including the algorithm for controlling the tip speed ratio (TSR) [2, 3], optimize torque (OT) [4, 5], and feedback power signal (PSF) [6], and methods using electrical signal as perturb and observe (P&O) [7, 8], optimal relationship based (ORB) [9, 10], these solutions have quick processing in the event of sudden wind changes is very susceptible to fluctuations around MPP. Therefore, intelligent algorithms have been applied to better handle these fluctuations and track the reference value more closely, these controllers are swarm optimization algorithms (SOA) [11], Fuzzy logic control (FLC) [12], neural network (NN) [13] or artificial neural network (ANN) [14]. A group of intelligent algorithms demonstrates outstanding capabilities in tracking reference values, but the mathematical model is quite complex and requires many sensors to provide external signals. SMC, which is not a novel control method, is one of the intelligent algorithms that can manage nonlinear systems and precisely track reference values. It also efficiently and steadily handles nonlinear problems when there are abrupt external disturbances like wind speed. Therefore, this study proposes the SMC based on MFC to MPPT for WECS.

2. Mathematical modelling of WECSs

The WECS is shown in Figure 1. On the left side of the PMSG is the mechanical conversion part, while on the right side is the electrical conversion part. When the wind speed exceeds 3 m/s, the turbine blades start rotating and drive the generator. The rated speed depends on the type of wind turbine and typically ranges from 15 to 18 m/s. When the wind speed is below the cut-in threshold or above the rated speed, the turbine blades are locked to protect the system.

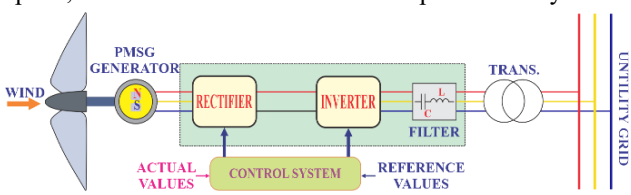

Figure 1. *Diagram of WECS using PMSG*

Accordingly, four operating regions can be defined: Region 1 with wind speeds lower than 3 m/s, Region 2 with wind speeds between 3 m/s and the rated speed, Region 3 at the rated wind speed, and Region 4 with wind speeds above the rated speed. Therefore, the MPP tracking process is only performed in Region 2, where the pitch angle of the wind turbine blades is set to $\beta = 0$.

2.1. Modelling of wind turbine

The wind turbine's aerodynamic power [12].

$$P_{aero} = \left[\rho.\pi.R_{wing}^2.C_p\left(\lambda,\beta\right).v_w^3\right]/2 \quad (1)$$

In which, v is the wind speed, R_{wing} is the radius of the blade, ρ is the air density and $C_p(\lambda,\beta)$ is the power coefficient as a nonlinear function of the blade's tip ratio λ and the angle of rotation β. The TSR is defined.

$$\lambda = \left(\omega_{tb}.R_{wing}\right)/v_w \quad (2)$$

ω_{tb} is angular velocity, reference angular velocity as:

$$\omega_{tb,ref} = \left(\lambda_{opt}.v_w\right)/R_{wing} \quad (3)$$

2.2. Mathematical model PMSG

Based on [13], the mathematical model for PMSG is as,

$$\begin{cases} d\omega/dt = \left(-B_v.\omega - T_e + T_a\right)/J \\ di_q/dt = -\left(R_g.i_q\right)/L_g - N.\omega.i_d - \left(\phi_m.N.\omega\right)/L_g + V_q/L_g \\ di_d/dt = -R_g.i_d/L_g + N.\omega.i_q + V_{ds}/L_g \end{cases} \quad (4)$$

The q-axis and d-axis currents are represented by i_q and

i_d, whereas voltages are V_q and V_d; the aerodynamic torque, T_{aero}; N is the pole pairs number; R_g is the resistor stator; $L_g = L_q = L_d$ are the inductances of the stator; J is the torque of inertia; B_v is viscous friction coefficient, Φ_m and T_e are magnetic flux linkage, and electromagnetic torque.

The electromagnetic torque is established as [11],

$$T_e = M.i_{qs} \tag{5}$$

where $M = 3/2.\phi_m.N$

Considering the disturbance of the resistance and inductance, as well as the noise and system model errors, the mathematical model of the PMSG is revised as follows,

$$\begin{cases} d\omega/dt = \left(-B_v.\omega - T_e + T_a\right)/J \\ di_q/dt = -\left(R_g.i_q\right)/L_g - N.\omega.i_d - \left(\phi_m.N.\omega\right)/L_g + V_q/L_g + d_q \\ di_d/dt = -R_g.i_d/L_g + N.\omega.i_q + V_{ds}/L_g + d_d \end{cases} \tag{6}$$

The terms d_q, d_d representing include modeling errors, uncertain parameters, noise and are defined,

$$\begin{cases} d_q = \left(R_g/L_g - R_{sum}/L_{sub}\right)T_e + \left(1/L_g - 1/L_{sub}\right)\phi_m.N.M.\omega \\ +M.V_q + \Delta_{qn} \\ d_d = \left(R_g/L_g - R_{sum}/L_{sub}\right)i_d + \left(1/L_g - 1/L_{sub}\right)V_d + \Delta_{dn} \end{cases} \tag{7}$$

Here, $R_{sum} = R_g + \delta R_g$ and $L_{sub} = L_g - \delta L_g$, with δR_g is the variable increase of resistance that can rise up to 40% and δL_g is the varying reactance of the inductor that can be reduced to 15%; meanwhile Δ_{qn}, Δ_{dn} corresponding to the noise and the modeling errors of the system [14], this value determines a sufficiently smooth and is bounded and the selected value $\Delta_{qn} = \Delta_{dn} = 10^5 \sin(t)$. Based on that, the error of the dynamic model is introduced as follows,

$$\begin{aligned} &\tilde{\omega} = \omega_{tb} - \omega_{tb,ref}, \omega_{tb,ref} = \lambda_{opt}.v.n_{gb}/R_{wing} \\ &\tilde{T}_e = T_e - T_{e,ref} = T_{aero}/n_{gb} - B_v.\omega_{tb,ref} - J.\dot{\omega}_{tb,ref} \end{aligned} \tag{8}$$

3. Model Free - Sliding mode controll

This section will discuss MFC and SMC algorithms.

3.1. Ultra-local mode and Mode Free control

When considering the changes of a system that includes a single input and output (SISO), it can be defined [15].

$$y^n = F + \gamma.u_c \tag{9}$$

In which, y^n is the *n-th* derivative of the system's output value, F is the total of the known and unknown parameters and $\gamma \in R$ is a non-physical parameter.

Normally, when $n = 1$, the interpretation of MFC will be represented in Figure 2 as described below,

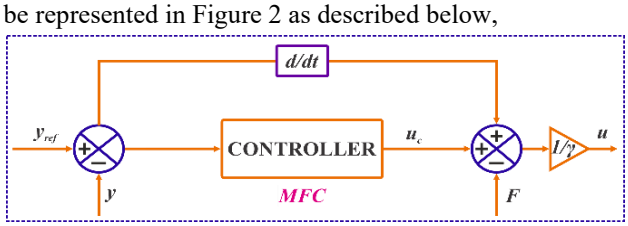

Figure 2. *Diagram of MFC modeling*

$$u = \left(-F + \dot{y}_{ref} + u_c\right)/\gamma \tag{10}$$

In that, u_c is the output signal of the controller, $\dot{y}_{ref}$ is reference value, F is the disturbance and uncertainties.

Transform the first and second equations in (6) to create new variables x and x_{ref} based on the T_a and ω_{tb}.

$$x = \kappa.\omega_{tb} + \tau \text{ and } x_{ref} = \kappa.\omega_{ref} + \tau \tag{11}$$

with $\tau = \dot{\omega}_{tb}$ and κ is selected as constant so that $\kappa > 0$.

By taking the derivative of (11), we have new equation.

$$\begin{aligned} \dot{x} &= \left(\kappa - B_v/J\right)\tau + \left(R_g.T_e\right)/\left(J.L_g\right) + \left(N.M.\omega_{tb}.i_d\right)/J \\ &+ \left(\phi_m.N.M.\omega_{tb}\right)/\left(J.L_g\right) + \dot{T}_a/J - \left(M.V_q\right)/\left(J.L_g\right) - d_q/J \end{aligned} \tag{12}$$

By combining equations (10) and (12), the loop for the angular velocity and aerodynamic torque is determined.

$$\dot{x} = F_1 + \gamma_1.V_q \tag{13}$$

Here, F_1 and γ_1 they have values as follows,

$$\begin{aligned} &\gamma_1 = M/J.L_g \text{ and} \\ &F_1 = \left(\kappa - B_v/J\right)\tau + \left(R_g.T_e\right)/\left(J.L_g\right) + \left(N.M.\omega_{tb}.i_d\right)/J \\ &+ \left(\phi_m.N.M.\omega_{tb}\right)/\left(J.L_g\right) + \dot{T}_a/J - d_q/J \end{aligned} \tag{14}$$

Based on the diagram in Figure 2 and combining (13), the control voltage values for q-axis V_q as.

$$V_q = \left(-F_1 + \dot{x}_{ref} + u_{qc}\right)/\gamma_1 \tag{15}$$

Similarly, set the MFC loop control variable for the current i_d, using the third equation of (6)

$$\dot{i}_d = F_2 + \gamma_2.V_d \tag{16}$$

In which, F_2 and γ_2, these are their values,

$$\gamma_2 = 1/L_g \text{ and } F_2 = R_g.i_d/L_g + N.\omega_{tb}.T_e/M + d_d \tag{17}$$

Using the control value setting rule as (13), we have,

$$V_d = \left(-F_2 + i_{d,ref} + u_{dc}\right)/\gamma_2 \tag{18}$$

Note, the initial condition of the reference current value d-axis is equal to 0 or $i_{d,ref} = 0$.

3.2. Design MFSMC controller

Error in angular velocity and aerodynamic torque loop,

$$\tilde{x} = x_{ref} - x \tag{19}$$

The derivative of (19), combined (9) and (10) for e_1

$$\dot{\tilde{x}} = \dot{x}_{ref} - \dot{x} = -u_{qc} \tag{20}$$

Choose sliding surface for traditional SMC.

$$s_1 = \dot{\tilde{x}} + \eta_1\tilde{x} \tag{21}$$

In that, η_1 is chosen as a positive constant.

The derivative (21) and substituting (20) gives us.

$$\dot{s}_1 = -\eta_1 u_{qc} + \ddot{\tilde{x}} \tag{22}$$

The SMC approach is chosen according to the geometric progression rule [17 18].

$$\dot{s}_1 = -h\,sgn\left(s_1\right) - ks_1 \tag{23}$$

Where h and k are defined as constants.

Confirm 1. When SMC is chosen (21) and the approach law is as (23), the control law is determined as.

$$u_{qc} = \left(\ddot{\tilde{x}} + h\,sgn(s_1) + ks_1\right)/\eta_1 \quad (24)$$

At that time, the state error of speed will gradually converge to 0 within a finite time.

Replace (24) with (15) to determine the value of the voltage control that regulates T_a and ω.

$$V_q = \left(-F_1 + \dot{x}_{ref}\right)/\gamma_1 + \left(\ddot{\tilde{x}} + h\,sgn(s_1) + ks_1\right)/(\gamma_1.\eta_1) \quad (25)$$

The V_q block diagram is illustrated as Figure 3.

Next, set the loop current error value i_d

$$\tilde{i}_d = i_{d,ref} - i_d \quad (26)$$

The derivative of (26), combining (16) and (18) for e_2

$$\dot{\tilde{i}}_d = \dot{i}_{ds,ref} - \dot{i}_{ds} = -u_{dc} \quad (27)$$

Choose a sliding surface for traditional SMC.

$$s_2 = \ddot{\tilde{i}}_d + \eta_2 \dot{\tilde{i}}_d \quad (28)$$

In that, η_2 is chosen as a positive constant.

Next, take the derivative of (28) and replace (27) into

$$\dot{s}_2 = -\eta_2 u_{dc} + \dddot{\tilde{i}}_d \quad (29)$$

The SMC approach is chosen according to the geometric progression rule [17 18].

$$\dot{s}_2 = -h\,sgn(s_2) - ks_2 \quad (30)$$

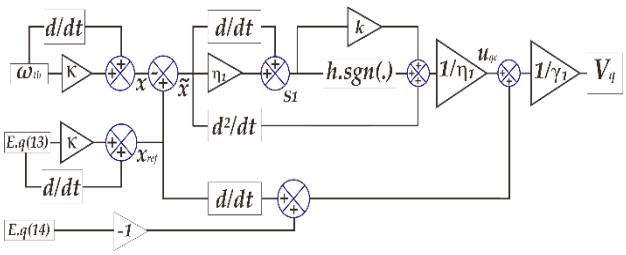

Figure 3. *Block diagram of V_q voltage*

Confirm 2. When SMC is chosen (28) and the approach law as (30), the control law is determined as,

$$u_{dc} = \left(\ddot{\tilde{i}}_d + h\,sgn(s_2) + ks_2\right)/\eta_2 \quad (31)$$

At that time, the state error of speed will gradually converge to 0 within a finite time.

Replace (31) with (18) the voltage value for the controller of the current the d-axis is determined as.

$$V_d = \left(-F_2 + i_{d,ref}\right)/\gamma_2 + \left(\ddot{\tilde{i}}_d + h\,sgn(s_2) + ks_2\right)/(\gamma_2.\eta_2) \quad (32)$$

The flowchart of V_q is illustrated as Figure 3 and the flowchart of V_d is illustrated as Figure 3.

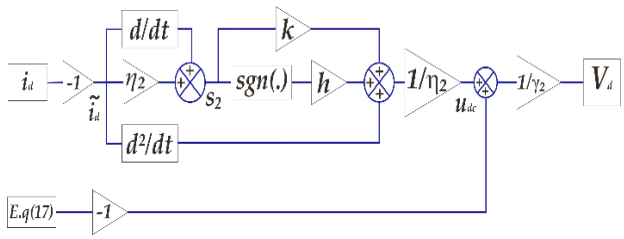

Figure 4. *Diagram of V_d voltage*

4. Simulation results on MATLAB - SIMULINK

The parameters of WECS and the controllers is introduced in Table 1 and Table 2.

Table 1. *WECS's parameter*

Symbol	Parameter	Value	Unit
P_{rate}	Rated power of the PMSG	5	kW
ω_{rated}	Rated speed of the PMSG	42	rad/s
N	Pole pairs	14	-
L_s	Inductance of the stator	3.55	mH
R_s	Resistance of the stator	0.3676	V.s/rad
Φ_m	Magnetic flux linkage	0.2867	kg·m^2
J	Inertia of the rotor	7.856	kg·m^2
B_v	Viscous friction coefficient	0.002	kg·m^2/s
Wind turbine parameter			
R	Turbine rotor radius	3	m
v_{rate}	Rate wind speed	12.5	m/s
-	Rate rotational speed	310	rpm
ρ	Air density	1.25	kg/m3

Table 2. *Parameter of controllers*

Controller	Parameter
1. Linear quadratic (LQ) optimal controller	Q = diag(2e5,1,1). T = 1e-2*diag(1,1,1).
2. Model free sliding mode controller (MFSMC)	κ =1e2; $\eta_1 = \eta_2 = 100$ h = 150; k = 1e3

Figure 5 shows steps to design the MFSMC controller

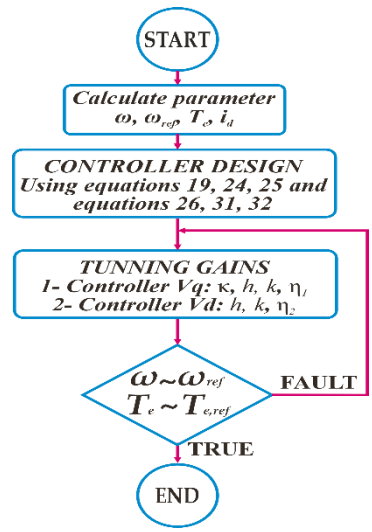

Figure 5. *Steps of design MFSMC controller*

The power of PMSG is 5kW, and the wind speed varies from 9-16m/s described in Figure 6.

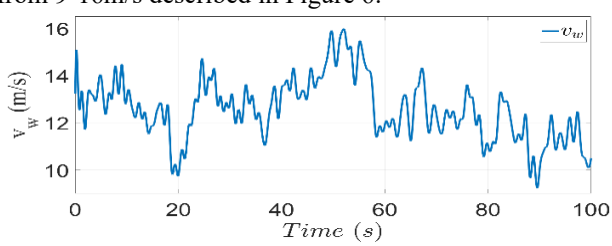

Figure 6. *Simulated average wind speed v_{rate} of 12.96 m/s*

The parameters of the WECS are reused according to [18], as shown in Table 1. When considering the MPPT of

WECS, ω and T_e, are compared with their reference values. The smaller the average error values, the greater the energy extraction capability of the controller, these two evaluation parameters include $e_{\omega,mean} = \left|\tilde{\omega} / \omega_{ref}\right|$ (with $e_{\omega} = \tilde{\omega}$) to evaluate the ability of the rotor to track reference value and $e_{T_{e,mean}} = \left|\tilde{T}_e / T_{e,ref}\right|$ (with $e_{T_e} = \tilde{T}_e$) evaluate the tracking ability of $T_{e,ref}$; in addition, there are parameters to evaluate the voltage supplied to the V_q controller with the q-axis.

From the results shown in the MATLAB - SIMULINK software in Figures 6 and 7 corresponding to two MPPT controllers using the LQR and the MFSCM.

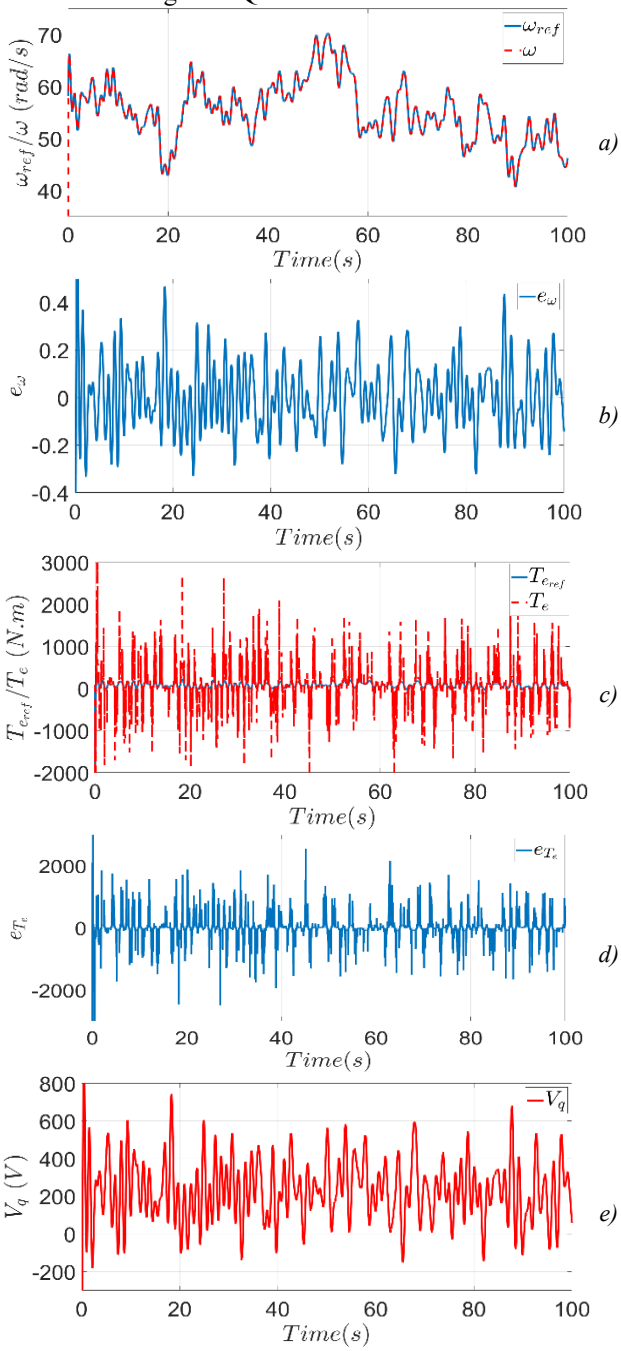

Figure 7. *a) The actual and reference angular velocity; b) The error of the angular velocity e_ω; c) The actual and reference value of the electromagnetic torque; d) The error deviation of e_{Te}; e) The q-axis voltage value V_q based on LQR controller*

From the values represented in Figure 7 corresponding to the LQR controller, the mean absolute deviation of the e_ω is 0.2069%; of e_{Te} is 95.9631%; mean of V_q is 280.8V, however, its value fluctuates at times exceeding 650V.

From the values represented in Figure 8 corresponding to the MFSMC controller, the mean absolute deviation of e_ω is 0.1439%; of e_{Te} is 16.9446%; the V_q is 274.3V and the control voltage is within the limit condition 650V.

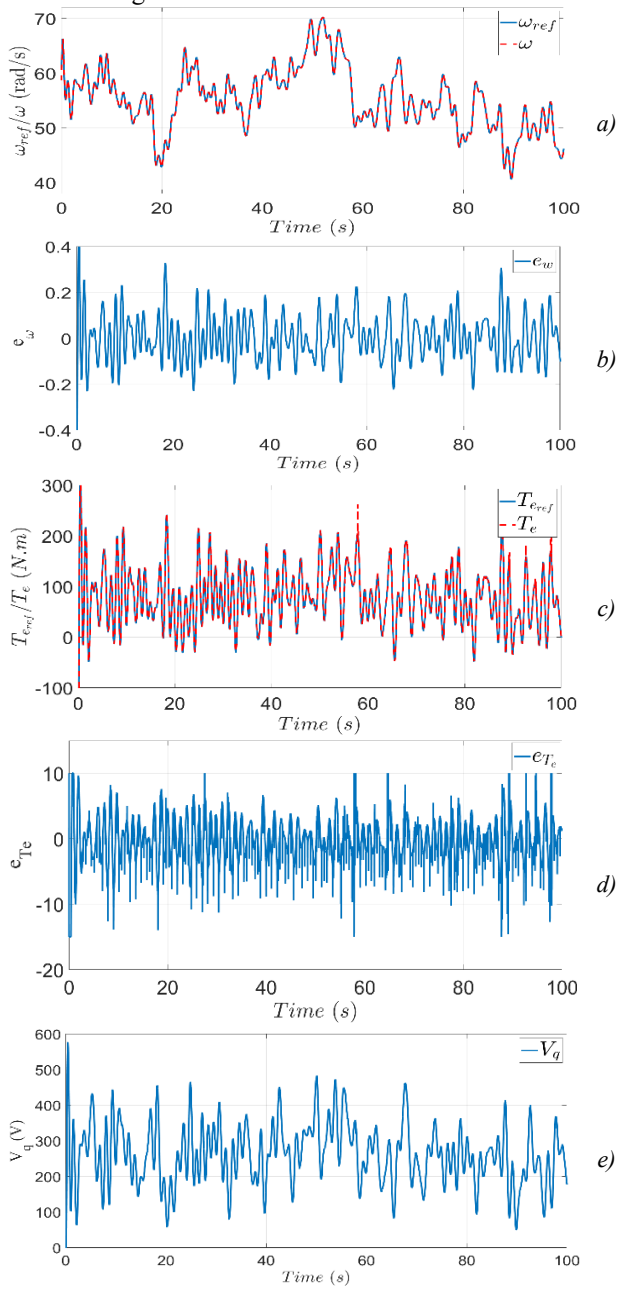

Figure 8. *a) The actual and reference angular velocity; b) The error of e_ω; c) The actual and reference value of the electromagnetic torque; d) The error deviation of e_{Te}; e) The q-axis voltage value V_q based on MFSMC controller*

5. Conclusion and development

Based on the simulation results presented in Figures 7 and Figure 8, these results show that the MFSMC controller is capable of tracking the reference values. It can be observed that the variations of the SMC effectively

nonlinear problems, and in this research, it can be evaluated that the quality of MPPT of MFSMC is better, and the voltage supplied to the controller is also low, indicating that the proposed controller save more energy than the LQR controller.

However, this research direction has not specifically addressed the disturbance factors of the system as well as the modeling errors; therefore, the next research direction needs to add observation sets to evaluate the changes in disturbances affecting the controller.

REFERENCES

[1] L. X. Chau, D. M. Quan, and L. K Hung, "Review of the modern maximum power tracking algorithms for permanent magnet synchronous generator of wind energy conversion system", *energies*, vol. 402, no. 16, pp. 1-25, 2023.

[2] C. M. Parker and M. C. Leftwich, "The effect of tip speed ratio on a vertical axis wind turbine at high Reynolds numbers", *Exp. Fluids*, vol. 57, p. 1–11, 2016.

[3] M. Nasiri, J. Milimonfared, and S. H. Fathi, "Modeling, analysis and comparison of TSR and OTC methods for maximum power point tracking and power smoothing in PMSG-based wind turbines", *Energy Convers. Manag*, vol. 86, p. 892–900, 2014.

[4] M. Yin, W. Li, C. Y. Chung, L. Zhou, Z. Chen, and Y. Zou, "Optimal torque control based on effective tracking range for MPPT of wind turbines under varying wind conditions", *IET Renew. Power Gener*, vol. 11, p. 501–510, 2017.

[5] X. Zhang, Y. Zhang, S. Hao, L. Wu, and W. Wei, "An improved MPPT method based on decreasing torque gain for large scale WT at low wind sites", *Electr. Power Syst. Res*, vol. 176, 2019.

[6] A. Mirecki, X. Roboam, and F. Richardeau, "Comparative study of maximum power strategy in wind turbines", *IEEE Int. Symp. Ind. Electron*, vol. 2, p. 993–998., 2004.

[7] M. A. Abdullah, A. H. M. Yatim, C. W. Tan, and A. S. Samosir, "Particle Swarm Optimization-Based Maximum Power Point Tracking Algorithm for WECS", *IEEE International Conference on Power and Energy (PECon)*, 2012, pp. 65-70.

[8] H. Mousa, A. Youssef, and E. Mohamed, "Modified P&O MPPT algorithm for optimal power extraction of five-phase PMSG based wind generation system", *SN Appl. Sci*, vol. 8, pp. 838-854, 2019.

[9] M. Kesraoui, N. Korichi, and A. Belkadi, "Maximum power point tracker of wind energy conversion system", *Renew. Energy*, vol. 36, p. 2655–2662., 2011.

[10] C. Carrillo, A. F. O. Montaño, J. Cidrás, and E. Díaz-Dorado, "Review of power curve modelling for wind turbines", *Renew. Sustain. Energy Rev*, vol. 21, p. 572–581, 2013.

[11] B. Wu, Y. Lang, N. Zargari, and S. Kouro, *Power Conversion And Control Of Wind Energy Systems*, Hoboken, New Jersey, A John Wiley & Sons, Inc., Publication, 2011, pp. 28-29.

[12] M. L. Corradini, G. Ippoliti, and G. Orlando, "Robust control of variable-speed wind turbines based on an aerodynamic torque observer", *IEEE Trans. Control Syst. Technol*, vol. 21, no. 4, pp. 1199-1206, Jul. 2013.

[13] O. Wallmark, "*On Control of Permanent-Magnet Synchronous Motors in Hybrid-Electric Vehicle Application*" Gothenburg, Sweden, Chalmers University of Technology, 2004.

[14] D. D. Ton and L. A. Vu, "High-order observers-based LQ control scheme for wind speed and uncertainties estimation in WECSs", *Optim Control Appl Meth*, vol. 39, p. 1818–1832, 2018.

[15] J. C. Fliess, "Model-free control", *Internat J Control*, vol. 86, no. 12, p. 2228–52, 2013.

[16] C. Fallaha, M. Saad, H. Kanaan, and K. Al-Haddad, "Sliding-Mode Robot Control With Exponential Reaching Law", *IEEE Trans.Ind. Electron*, vol. 58, p. 600–610, 2011.

[17] S. Su, H. Wang, H. Zhang, Y. Liang, and W. Xiong, "Reducing Chattering Using Adaptive Exponential Reaching Law", *2010 Sixth International Conference on Natural Computation (ICNC 2010)*, 2010, pp. 1-4.

[18] D. D. Ton, "Disturbance Observer-Based Fuzzy Sliding Mode Control of WECSs Without Wind Speed Measurement", *IEEE Access*, vol. 5, pp. 1-9, 2017.